© 2017. Published by The Company of Biologists Ltd | Journal of Experimental Biology (2017) 220, 194-207 doi:10.1242/jeb.145094

RESEARCH ARTICLE

Barnacle biology before, during and after settlement and metamorphosis: a study of the interface

Tara Essock-Burns[1,*], Neeraj V. Gohad[2], Beatriz Orihuela[3], Andrew S. Mount[3], Christopher M. Spillmann[4], Kathryn J. Wahl[5] and Daniel Rittschof[3]

ABSTRACT

Mobile barnacle cypris larvae settle and metamorphose, transitioning to sessile juveniles with morphology and growth similar to that of adults. Because biofilms exist on immersed surfaces on which they attach, barnacles must interact with bacteria during initial attachment and subsequent growth. The objective of this study was to characterize the developing interface of the barnacle and substratum during this key developmental transition to inform potential mechanisms that promote attachment. The interface was characterized using confocal microscopy and fluorescent dyes to identify morphological and chemical changes to the interface and the status of bacteria present as a function of barnacle developmental stage. Staining revealed patchy material containing proteins and nucleic acids, reactive oxygen species amidst developing cuticle, and changes in bacteria viability at the developing interface. We found that as barnacles metamorphose from the cyprid to juvenile stage, proteinaceous materials with the appearance of coagulated liquid were released into and remained at the interface. It stained positive for proteins, including phosphoprotein, as well as nucleic acids. Regions of the developing cuticle and the patchy material itself stained for reactive oxygen species. Bacteria were absent until the cyprid was firmly attached, but populations died as barnacle development progressed. The oxidative environment may contribute to the cytotoxicity observed for bacteria and has the potential for oxidative crosslinking of cuticle and proteinaceous materials at the interface.

KEY WORDS: Antimicrobial, Fouling, Confocal, Attachment, Bacteria, Reactive oxygen species

INTRODUCTION

Barnacles have a complex life cycle involving drastic changes from a planktonic free-swimming nauplius and cypris larva, to a sessile juvenile barnacle with adult morphology (Crisp, 1955; Crisp and Meadows, 1963; Barnes and Blackstock, 1974; Aldred and Clare, 2008; Gohad et al., 2012; Maruzzo et al., 2012). Adhesion is critical for survival during the transition from cyprid to juvenile and necessary to maintain permanent attachment as the juvenile grows into an adult. Mechanisms of barnacle attachment via fluids that undergo curing have garnered scientific interest for applications to control biofouling in industrial (Callow and Callow, 2002; Holm, 2012) and medical contexts (Shivapooja et al., 2013) and bioinspired glues that cure in aqueous environments (Joseph et al., 2011; Kamino, 2013). First, the barnacle cyprid attaches to the substratum via a permanent adhesive, released from cement glands through the two walking appendages, a pair of antennules, embedding them completely, creating an adhesive plaque that anchors them in place (Knight-Jones and Crisp, 1953; Crisp, 1960; Walker, 1971, 1973; Yule and Walker, 1985; Mullineaux and Butman, 1991; Matsumura et al., 1998; Phang et al., 2008; Gohad et al., 2012, 2014; Aldred et al., 2013). The subsequent phases of settlement and metamorphosis for acorn (balanomorph) barnacles involve major changes to the body plan and shape, resulting in a disk-shaped basis parallel to the substratum as a juvenile. Later, the shell plates become calcified and the barnacle continues to expand its basis and side plates as the animal grows and molts throughout its life. This critical transition from cyprid to juvenile and the ability to interface with diverse substrata in order to permanently attach is important to understanding the biology that influences barnacle adhesion.

Extensive literature describes barnacle settlement in response to various natural product and biofilm stimuli; however, unlike for other marine biofouling larvae (Hadfield, 1986, 2011; Pawlik and Hadfield, 1990; Unabia and Hadfield, 1999), the role of biofilms in inducing or inhibiting barnacle settlement is complex and larvae will ultimately settle on surfaces regardless of the biofilm state (Rittschof et al., 1986; Maki et al., 1988, 1989, 2000; Dobretsov et al., 2006; Khandeparker et al., 2006). Chemical cues indicating the presence of other barnacles are the strongest driver of larval settlement (Knight-Jones and Stevenson, 1950; Knight-Jones and Crisp, 1953; Crisp and Meadows, 1963; Crisp, 1969; Matsumura et al., 1998; Dreanno et al., 2006a,b; Khandeparker and Anil, 2011). Thus, the assumption is that barnacles must utilize mechanisms to permanently attach to substrata covered in a variety of biofilm communities. Much work has been done to characterize biofilm communities on common barnacle substrata (Dobretsov and Thomason, 2011) and on shell surfaces (Bacchetti De Gregoris et al., 2012); however, little is known of the interactions between barnacles and bacteria during and after settlement and metamorphosis.

The composition of barnacle secretions at each stage of attachment is crucial to understanding mechanisms that cement them to substrata. Initially, cyprids adhere using a heterogeneous mixture containing a proteinaceous bulk material (Hillman and Nace, 1970; Saroyan et al., 1970, 1996; Gohad et al., 2014), including phosphoprotein (Gohad et al., 2014), with an outer barrier (Walker, 1971) that contains lipid (Gohad et al., 2014). Juvenile attachment mechanisms have been less well studied, but it was found that a proteinaceous juvenile cement appears to increase

[1]Kewalo Marine Laboratory, Pacific Biosciences Research Center, University of Hawaii, 41 Ahui St, Honolulu, HI 96813, USA. [2]Okeanos Research Group, Department of Biological Sciences, 132 Long Hall, Clemson University, Clemson, SC 29634, USA. [3]Duke University Marine Laboratory, Marine Science and Conservation, 135 Duke Marine Lab Road, Beaufort, NC 28516, USA. [4]Center for Bio/Molecular Science and Engineering, Naval Research Laboratory, Washington, DC 20375, USA. [5]Chemistry Division, Naval Research Laboratory, Washington, DC 20375, USA.

*Author for correspondence (essock@hawaii.edu)

T.E.-B., 0000-0003-4159-6974

Received 22 June 2016; Accepted 18 October 2016

Journal of Experimental Biology

Journal of Experimental Biology (2017) 220, 194-207 doi:10.1242/jeb.145094

adhesion within 2 weeks of settlement and metamorphosis (Yule and Walker, 1984), earlier than the adult cement system is known to develop (40 days later) (Walker, 1973). Much later, adult barnacles use a combination of mostly proteinaceous secretions (Walker, 1971; Burden et al., 2012, 2014), which become insoluble over time (Kamino et al., 1996; Naldrett and Kaplan, 1997; Kamino, 2001; Dickinson et al., 2009).

In terms of direct interaction between barnacle adhesives and bacteria on a surface, previous work observed bacteria surrounding the adhesive plaque, which forms during the initial stage of settlement (Aldred et al., 2013), suggesting that bacteria may be attracted to and excluded from the adhesive material. Additionally, it was found that partially metamorphosed juveniles adhere more strongly on biofilm-coated surfaces than on clean ones, but found no difference in adhesion strength for completely metamorphosed juveniles (Zardus et al., 2008), suggesting there may be something important about the interaction with biofilms at specific stages of settlement and metamorphosis for adhesion.

The developing adult barnacle basis contains overlapping layers of cuticle, which stretch, break and are augmented by newer bands during growth (Bocquet-Vedrine, 1965; Bourget and Crisp, 1975; Crisp and Bourget, 1985). Recent insight into the interfacial fluids of barnacles revealed two distinct secretions differing spatiotemporally as the adult barnacle grows, one released at the periphery and the other delivered periodically via the network of capillaries and ducts (Burden et al., 2012) connected to the cement gland (Yule and Walker, 1987). In this study, our driving question was: how does the interface between the barnacle and the substrate change during the morphological transition of cyprid to juvenile? To address this question, we combined confocal microscopy and specific fluorescent dyes to examine the spatiotemporal distribution of the secretions and bacteria in the developing interface for cyprid larvae prior to settlement, at all stages during settlement and metamorphosis, and for juvenile barnacles up to 7 days after settlement. In the present study, both the transformation of the interface between the barnacle and substratum and the presence and viability of bacteria during those developmental stages was explored. We also investigated the oxidative environment by assessing reactive oxygen species (ROS) as potentially active antimicrobial and/or crosslinking agents at the interface during settlement and metamorphosis.

MATERIALS AND METHODS

Collection of cypris larvae and juveniles from the field or rearing of cypris larvae

Larvae of *Amphibalanus (=Balanus) amphitrite* Darwin 1854 were used, which were either reared in the laboratory or collected from plankton at the Duke University Marine Laboratory in Beaufort, NC, USA. Nauplii released from mature adults collected from the field were raised following established culture techniques (Rittschof et al., 1984, 1992, 2008; Holm, 1990). For comparison with animals from the field, cyprids were sorted from plankton collected off the Duke Marine Laboratory docks using a 64 µm mesh plankton net in June 2013. To collect juveniles from the field, coverslips were secured to plastic rulers with clear rubber bands and the rulers were tethered with zip ties to PVC pipes from a floating dock, submerged ∼30 cm under the surface. The rulers were checked daily for barnacle settlement and four juveniles were collected and fixed for comparison with the lab-reared juveniles, as described below. For most experiments, cultured cyprids were used and settled in the lab.

Settlement

Barnacles were examined in seven groups spanning the entire transition from cyprid to juvenile before, during and after settlement and metamorphosis. Cyprids were settled and allowed to develop through the six stages previously defined via morphological characteristics (Maruzzo et al., 2012). In accordance with previously established techniques, cyprids were aged for 3 days in aged filtered seawater (FSW) at 4°C prior to settlement (Rittschof et al., 1984, 1992). The aged filtered seawater was passed through four spools of polypropylene thread, 5 µm filter size, and aged for at least 2 weeks prior to use; this aged FSW contains an estimated bacterial load of $0.53(\pm0.04)\times10^6$ cells ml^{-1}, which is half as much bacteria as non-aged FSW [$1.11(\pm0.17)\times10^6$ cells ml^{-1}]. Coverslips (Fisherbrand Microscope cover glass 12-541-B, 22×22–1.5 mm) were briefly flamed, then cooled to room temperature and a circle was drawn with a wax pencil to retain the seawater drop. Using a pipette, approximately 6–12 cyprids were placed in a small drop of aged FSW (∼1 ml). Coverslips with larvae were housed individually in Falcon® 1006 polystyrene Petri dishes in a 28°C incubator and observed and sampled as larvae underwent settlement and metamorphosis. We used the six stages following previous descriptions, but combined stages 3–5 into one group, as those transitions occur too rapidly to detect without video observation, which was how they were originally described (Maruzzo et al., 2011, 2012). In brief, stage 1 corresponded to cyprids immediately after irreversible attachment and stage 2 was a cyprid with the carapace drawn closer to and in parallel with the surface (Maruzzo et al., 2012). Stages 3–5 included significant changes in morphology; first, the larva became a small ball within the cypris carapace; then, it formed a larger bag-like body shape (Maruzzo et al., 2012). Stage 6 was a fully metamorphosed juvenile with a fully shed cypris carapace and compound eyes, in the shape of an adult with visible shell plates (Maruzzo et al., 2012). In addition to the four groups observed during the transition from cyprid to juvenile, this study included one group of free-swimming cyprids prior to settlement, and two groups of juveniles that were 3–5 and 6–7 days old following completion of settlement and metamorphosis (stage 6). About 218 barnacle larvae were examined in total, from 10 separate batches of larvae, with the majority as stage 6 (N=153), newly metamorphosed juveniles (Table 1), as this stage of development was the primary focus of the study.

All barnacles were eventually fixed in 4% buffered paraformaldehyde (pH 7.5–8) in phosphate-buffered saline solution (PBS; 10× PBS: 80 g NaCl, 2 g KCl, 14.4 g Na_2HPO_4, 2.4 g KH_2PO_4 in 1 l nanopure water, stirred without heat until dissolved), made fresh at each time of fixation. Cyprid samples were incubated in 10% w/v $MgCl_2$ in aged filtered seawater for 10–15 min prior to fixing in 4% buffered paraformaldehyde (pH 7.5–8), so that the antennules remained extruded. Pre-settlement cyprids were observed in 8-welled chambered slides (ThermoFisher Scientific cat. no. 155409PK) with no. 1.5 coverslip bottom, kept in aged FSW to avoid physically damaging them during confocal microscopy. Coverslips with attached barnacles were kept in 50 ml capped tubes completely submerged in fixative (∼15 ml), and stored at 4°C for 1 day up to 2 months prior to staining and imaging.

Staining

Prior to staining, samples were washed three times with 1× PBS, made fresh from the 10× stock solution described above. For staining, coverslips were treated in individual Falcon® 1006 polystyrene Petri dishes. Barnacles in all groups were stained with fluorescent nucleic acid dyes to identify the presence, location and

Journal of Experimental Biology (2017) 220, 194-207 doi:10.1242/jeb.145094

Table 1. Summary of observations of barnacle larvae before, during and after settlement and metamorphosis using confocal microscopy (*N*=218), categorized in seven groups based on development

Group ID	Stage	Description	Bacteria	Patchy material
A	Cyprid Pre-settlement (*N*=8)	Pre-settlement larvae prior to surface exploration (lab and field)	None on carapace or extruded antennules	Not applicable
B	Stage 1 Early settlement (*N*=6)	Beginning of settlement, antennular adhesive released	When present (50%), a mixture of live and dead observed near antennules, mostly live	Adhesive plaque from antennules only, stains for protein and phosphoprotein
C	Stage 2 Mid-settlement (*N*=4)	Antennules retracted and cyprid body flattened and parallel to surface	Always present (100%), a mixture of live and dead observed near antennules, mostly live	Adhesive plaque from antennules only, stains for protein and phosphoprotein
D	Stages 3–5 Mid-late settlement (*N*=14)	Major changes in the body plan as metamorphosis begins and basis is formed	Often present (85%), a mixture of live and dead observed near antennules	Patchy material (59%) outside of antennule adhesive plaque and associated with cuticle
E	Stage 6 Late settlement/early juvenile (bacteria *N*=76; patchy material *N*=153)	Fully metamorphosed juvenile, with cyprid molt separated; autofluorescent cuticle appears disorganized; capillaries and ducts seldom observed (1/153)	Almost always present (92%) and mostly dead around antennule and live or mixture around cuticle	Patchy material (99%) outside of antennule adhesive plaque, associated with cuticle, and stains for protein and phosphoprotein; reactive oxygen species observed near antennules and cuticle
F	Day 3–5 Post-settlement (bacteria *N*=23; patchy material *N*=16)	Juvenile with more organized cuticle bands and one ring of capillaries and ducts observed (30%)	Always present (100%) and mostly dead around antennule and mixture around cuticle	Patchy material (88%) near antennule adhesive plaque, associated with the cuticle
G	Day 6–7 Post-settlement (*N*=10)	More organized cuticle bands and two rings of capillaries and ducts observed (20%)	Always present (100%) but concentrations less abundant, mostly dead	Patchy material (90%) near antennule adhesive plaque, associated with the cuticle

viability state of bacterial cells at the interface. BacLight LIVE/DEAD® (Life Technologies cat. no. L7007) bacterial viability kit was used, which contains a mixture of SYTO 9 (excitation 485 nm/emission 530 nm), a cell membrane-permeable nucleic acid dye, and propidium iodide (excitation 485 nm/emission 630 nm), a cell membrane-impermeable nucleic acid dye. The SYTO 9 dye stains all nucleic acids regardless of the state of the cell membrane, while the propidium iodide can only access nucleic acids when cell membranes are damaged (Boulos et al., 1999; Desjardins et al., 1999). In combination, they can be used to assess cell viability, where SYTO 9 staining indicates 'live' cells and propidium iodide staining indicates 'dead' cells (Boulos et al., 1999; Desjardins et al., 1999). Equal parts of stain were mixed in 1× PBS for a final concentration of 3 µl ml^{-1} of PBS. Samples with 1 ml of LIVE/DEAD stain per sample were incubated in the dark for approximately 20 min. Samples were washed twice with 1× PBS and kept in the dark prior to imaging, and were immersed in PBS during imaging.

The fluorescent probes used to determine whether the interface between the barnacle and the substrate contained protein and/or phosphoprotein were SYPRO® Ruby protein gel stain (excitation 460 nm/emission 620 nm) and Pro-Q® Diamond phosphoprotein stain (excitation 560 nm/emission 600 nm) (Life Technologies cat. no. S-12000 and P-33300). The SYPRO Ruby general protein stain protocol was adapted from the manufacturer' instructions; samples were incubated at room temperature in the dark for 5 h prior to PBS washes and imaging. Pro-Q Diamond stain for phosphoproteins was also developed for protein gels, but has been used for confocal scanning laser microscopy previously (Gohad et al., 2014); samples were incubated with the dye at room temperature in the dark for 1 h prior to PBS washes and imaging. Samples were stained with Pro-Q Diamond and imaged first and then washed and stained with SYPRO Ruby and imaged second, as instructed by the manufacturers. A subset of samples was only stained with SYPRO Ruby.

The CellROX® Orange fluorescent probe (excitation 545 nm/emission 565 nm; ThermoFisher Scientific cat. no. C10443) was used to determine the oxidative environment at the interface; unfixed (live barnacle) samples were stained for 30 min with dye at a final concentration of 5 µmol l^{-1} to ensure compatibility with the stain. The CellROX orange reagent fluoresces when oxidized and is used to indicate the presence of several ROS including: hydrogen peroxide, hydroxyl radical, nitric oxide, peroxynitrite anion and/or superoxide anion. Hoechst 33342 (excitation 350 nm/emission 461 nm; ThermoFisher Scientific cat. no. H3570), a cell membrane-permeable nucleic acid stain, was used in conjunction at 10 mg ml^{-1} and stained for 15 min.

Confocal microscopy

Confocal laser scanning microscopy was performed as described previously (Gohad et al., 2009, 2012, 2014; Aldred et al., 2013). Most images were taken using the Zeiss LSM 780 inverted confocal laser scanning microscope at Duke University equipped with laser lines of 405, 458, 488, 514, 561 and 633 nm. Additional imaging was performed using a Nikon C1si Spectral Confocal Imaging system at the US Naval Research Laboratory and a Nikon Ti-E inverted microscope equipped with a Nikon C1si Spectral Confocal Imaging system at Clemson University. FIJI (ImageJ) was used for most image processing and Imaris image analysis software (Bitplane Scientific Software) was used through the Duke University Light Microscopy Core Facility.

All manufacturer specifications were used for excitation and emission wavelengths for the fluorescent dyes with the exception of SYPRO Ruby, for which it was found that the specified optimal excitation peak of 460 nm was ineffective and a 405 nm excitation

Journal of Experimental Biology (2017) 220, 194-207 doi:10.1242/jeb.145094

was effective in this application. Laser power and gain settings were set to comparable ranges for all sets of dyes, but adjustments were made when needed to optimize signal to noise ratios for detection.

Quantification of bacteria

To estimate bacterial load in the aged seawater used, water samples were stained with SYTO 9 and filtered onto a 0.1 µm filter, and cells were counted per field of view under 100× objectives with a Nikon epifluorescence microscope. Aged (5 µm) filtered seawater samples were compared with non-aged filtered seawater and untreated estuarine seawater. For estimations of bacterial density observed at the interface of barnacles via confocal microscopy, three representative images for each stage of settlement were quantified (the minimum number of barnacles with bacteria observed at each stage). Using FIJI, one slice in the *Z*-direction in the SYTO 9 channel (total bacteria) was extracted from the stack and converted to a black and white image, and thresholds were applied to minimize cuticle and material and to only show dots of bacteria. Particles with an area of 0.5–3 µm were analyzed and counted. The density was calculated as the total number of particles per total area of the image. Means and s.e.m. are reported.

RESULTS

Bacteria at the interface

Barnacles in all groups of settlement and metamorphosis were examined using multiple nucleic acid stains except cyprids, for which only one dye was used (Hoechst 33342 was used for all stages including cyprids and SYTO 9 and propidium iodide were used on all stages except cyprids) and interfacial features are summarized in Table 1. The groups included: group A, pre-settlement cyprids (Fig. S1); groups B–E, settlement and metamorphosis stages 1, 2, 3–5 and 6 (Figs 1–4); group F, juveniles 3–5 days after completion of settlement and metamorphosis (Fig. 5); and group G, juveniles 6–7 days after settlement (Fig. S2). Pre-settlement cyprids (group A) lacked bacteria on the carapace or on antennules, including cyprids collected from the field (Table 1, Fig. 6; Fig. S1). The bacteria observed beginning at stage 1 through to day 6–7 after settlement and metamorphosis were similar in morphology, being 1–2 µm in length and rod shaped, and were often in doublets, possibly indicating the end of cell division (Fig. 2A,B). They were separate from the barnacle tissue and were first observed within a few micrometers of the surface of the coverslip. The bacteria showed a gradient of distribution, with areas of high density near the cyprid adhesive plaque and distributed more evenly throughout the rest of the area under the barnacle. The average density of bacteria was similar for stage 1 through to day 3–5 juveniles (Fig. 6C), ranging from 0.010±0.006 to 0.0142±0.008 cells µm^{-2}, whereas day 6–7 had the lowest density, at 0.003±0.001 cells µm^{-2} (Fig. 6C).

Barnacle stage 1 and stage 2 – early attachment and settlement

Bacteria were first observed at the interface of stage 1 barnacles (3/6 larvae), which coincides with the initiation of cyprid adhesive release via the antennules (group B; Figs 1A, 6A,B). Consistent with previous observations in early settlement, bacteria appeared surrounding the cyprid adhesive plaque (Gohad et al., 2012, 2014), but unlike previously, they were seen covering the edge of the cyprid antennules themselves, where they protruded from the adhesive plaque. Stage 2 barnacles (group C) had very similar features to stage 1 barnacles in terms of the cyprid adhesive plaque, and bacteria became more concentrated surrounding it (Figs 1B and 6). Other than autofluorescence of the antennules and parts of the carapace

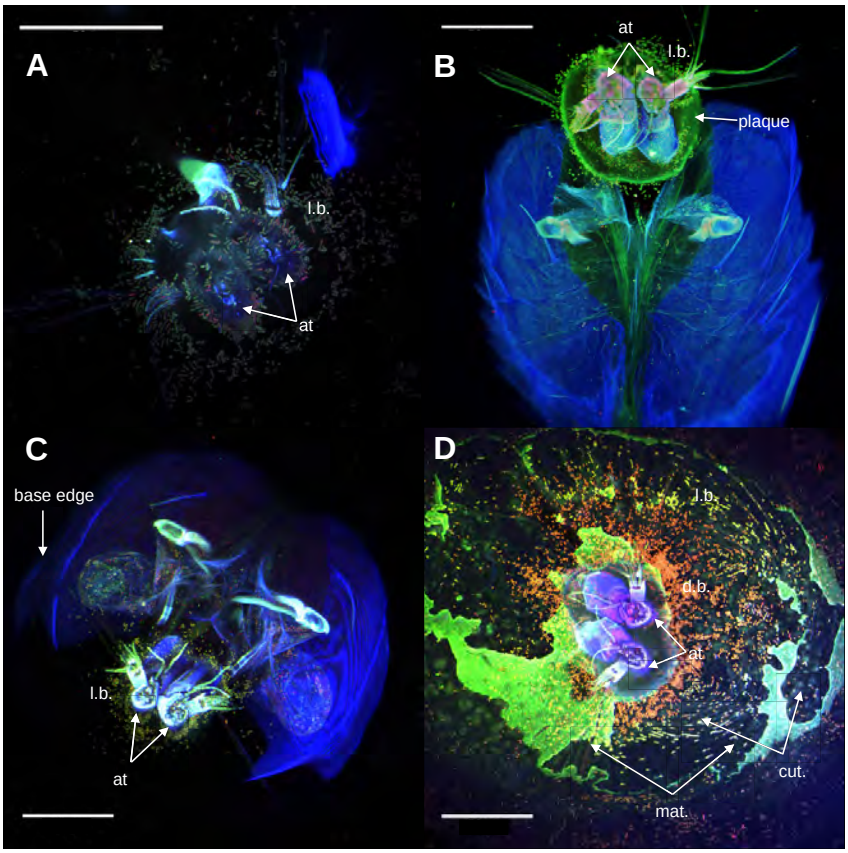

Fig. 1. The four stages of *Amphibalanus amphitrite* settlement. Representative confocal microscope images with SYTO 9/propidium iodide staining for live/dead bacteria and autofluorescence with 405 nm excitation. (A) Stage 1, paired antennules (at) are the only barnacle feature at the interface and are surrounded by mostly green dots indicating live bacteria (l.b.), with interspersed red dots indicating dead bacteria. (B) Stage 2, the paired antennules (at) are embedded in the adhesive plaque and surrounded by live bacteria (l.b.). Additional barnacle features are visible including the carapace (blue). (C) Stages 3–5, the barnacle body is rounded and condensed (edge of basis is visible). The paired antennules (at) are surrounded by live bacteria (l.b.). (D) Stage 6, the paired antennules (at) are embedded in the plaque, separating them from the densely packed dead bacteria (d.b.). The striations of autofluorescent cuticle form rings between the antennules and the edge (off of the image). A material new to the interface appears in irregular shapes between the plaque and the cuticle. Live bacteria (l.b.) are visible further from the antennules. Scale bars, 50 µm.

Journal of Experimental Biology (2017) 220, 194-207 doi:10.1242/jeb.145094

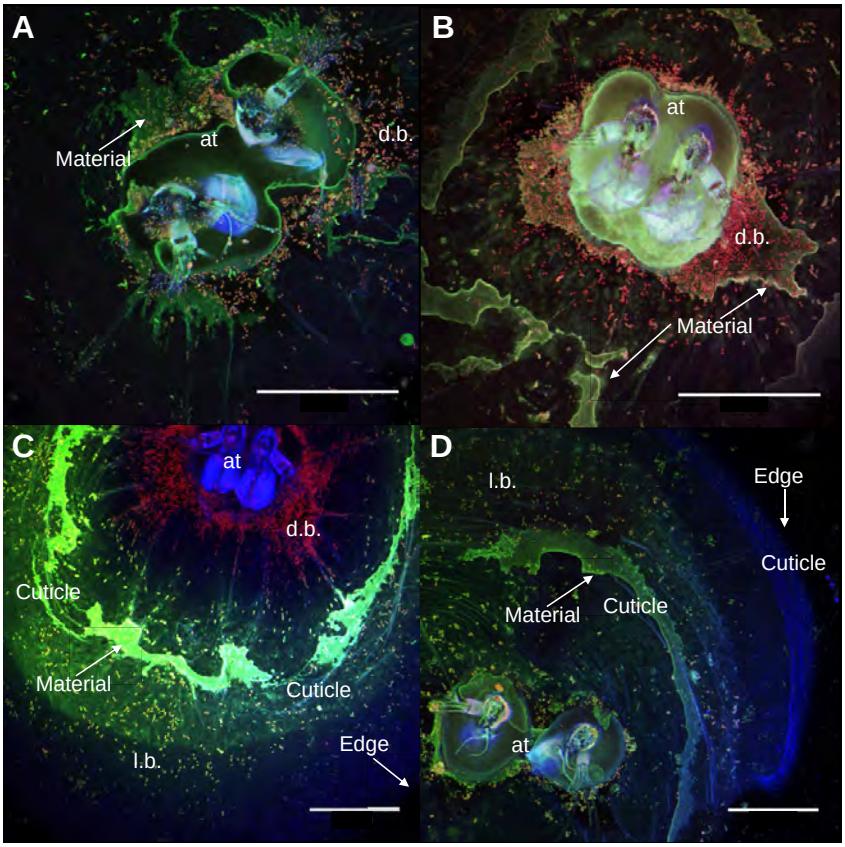

Fig. 2. Confocal microscope images of four stage 6 (newly metamorphosed juveniles) barnacles, near completion of settlement and metamorphosis. Paired antennules (at) are present (blue) and are embedded in the adhesive plaque (green). The patchy material (green) is visible near the antennules but exterior to the plaque (A,B) and amidst cuticle bands (C,D). Dead bacteria (d.b., red dots) were prominent around antennules, while live bacteria (l.b., green dots) were further away, associated with the cuticle (C,D) along with other dead bacteria. The edge of the barnacle is indicated, showing the cuticle and material occur halfway between the edge and the antennules. Scale bars, 50 μm.

within the observed range, no other materials or barnacle features were observed in these two stages (Fig. 1). After settlement was initiated (group B), bacteria were observed in 96% of all subsequent stages (Table 1, Figs 1 and 6).

Barnacle stages 3–5 – substantial changes in shape

The interface of metamorphosis stages 3–5 (group D) was markedly different from that of earlier stages (Table 1, Figs 1–4 and 6). Beginning at this time during barnacle development, there was evidence of a novel material at the interface, in addition to the cyprid adhesive plaque. The material was patchy and irregular in shape and observed in 59% of barnacles in this group (Fig. 6), made obvious by bright and diffuse staining with SYTO 9 (Figs 1–4). The location of the material was adjacent to the cyprid antennule adhesive plaque, but clearly distinct from it, demarcated by the plaque boundary (Figs 2–4).

Barnacle stage 6 – fully metamorphosed juvenile

The final stage of settlement and metamorphosis, stage 6, was marked by substantial changes at the interface in terms of the consistent presence of the patchy material, barnacle basis development, localization and viability of bacteria. The patchy material was observed in 152 out of 153 group E barnacles (Fig. 2). The material stained with both propidium iodide and SYTO 9 nucleic acid stains (Fig. 3), but was most obvious with the SYTO 9 stain (Figs 1D, 2 and 3A–C). It was not visible in unstained controls when excited with 405 nm light and broad emission settings, but seemed to weakly interact with the Hoechst 33342 nuclear stain. Because of overlap between Hoechst 33342 excitation and emission and the barnacle autofluorescence, we could not conclude whether Hoechst 33342 interacted with the material.

Barnacle day 3–5 and day 6–7 – post-metamorphic juveniles

Finally, older post-metamorphic juveniles that were 3–5 days (group F; Fig. 5) and 6–7 days old (group G; Fig. S2) showed similar features to stage 6 barnacles in terms of the presence of patchy material and dead bacteria, with the exception that the autofluorescent striations of the cuticle appeared more organized than previous stages. The overall density of bacteria was lower in the last stage examined, day 6–7 (Fig. 6C). The material seen in later stages of settlement and metamorphosis was also present in these older post-metamorphic juveniles. However, it was less expansive and confined to smaller areas associated with cuticle striations (day 3–5; Fig. 5; and day 6–7; Fig. S2). Also observed in the older juveniles was the formation of radial capillaries with ducts terminating at the basis (Fig. 5; Fig. S2). These highly fluorescent capillaries (when excited at 405 nm) were observed in one stage 6 barnacle (group E), and in 30% of day 3–5 post-settlement juveniles (group F; Table 1, Fig. 5), while two rings were observed in 20% of day 6–7 post-settlement juveniles (group G; Table 1 and Fig. S2). Out of 184 barnacles including group D (stage 3–5), when it first appeared, to group G (6–7 days after settlement), there were 174 (95%) barnacles with the patchy material at the interface (Table 1, Fig. 6).

New material at the interface

In general, the new interfacial material was observed in two regions: (1) adjacent to the adhesive plaque, usually within 20 μm of the antennules (Figs 1D, 2A,B), as was seen in stage 3–5 (group D), and (2) associated with the adjacent striations of cuticle, which were 30–100 μm lateral from the antennules (Figs 1D, 2B–D, 3 and 4). The material always spanned the depth of the interface (8–20 μm) and was physically in contact with the basis and the substratum (Fig. 4;

Journal of Experimental Biology (2017) 220, 194-207 doi:10.1242/jeb.145094

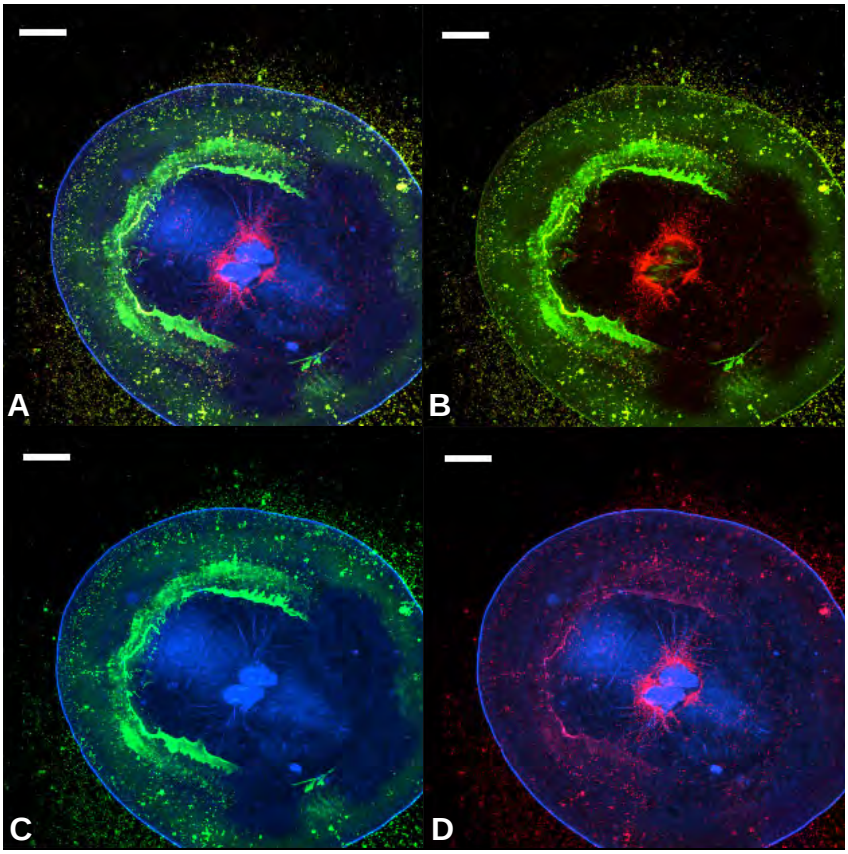

Fig. 3. Confocal microscope image of a newly metamorphosed juvenile (stage 6) showing the spatial organization of the stained interfacial material to the live and dead bacteria under the barnacle. SYTO 9/ propidium iodide staining showing antennules and the edge of the barnacle via autofluorescence (blue), live bacteria (green dots), dead bacteria (red dots) and patchy material (green and red) amidst rings of cuticle (blue lines). (A) Combined channels of broad-spectrum autofluorescence with 405 nm excitation and SYTO 9 and propidium iodide channels. (B) Channels for SYTO 9/ propidium iodide only. (C) Autofluorescence and SYTO 9. (D) Autofluorescence and propidium iodide. Scale bars, 50 μm.

Movie 1). The edge of the barnacle basis was often visible, but >20 μm above the substratum, and on the upper limit of the depth imaged (Figs 3, 4; Movie 1). The autofluorescent ring-like striations of the cuticle were prominent in stage 6 (Figs 1D, 2C,D and 4). The cuticle striations formed halfway between the antennules and the edge of the barnacle basis and appeared disjointed, and varied in the gap size between adjacent bands. Overall, bands of cuticle were much less uniform at this stage of newly metamorphosed juveniles (stage 6) than what was seen in older juveniles (day 3–5; Fig. 5; and day 6–7; Fig. S2).

Live/dead patterning of bacteria at the interface

Bacteria observed at the interface of early stages of settlement and metamorphosis, stage 1 through to stages 3–5, were ∼75% live and randomly mixed with dead bacteria as indicated by positive SYTO 9 staining and negative propidium iodide staining (Fig. 1A–C). Stage 6 barnacles (N=76) had different patterns of bacteria from previous stages. In terms of distribution, bacteria covered the entire area under the barnacle basis, but were especially dense surrounding the cyprid adhesive plaque. Additionally, there were two patterns of bacterial population viability. In about half of the stage 6 barnacles observed, the bacteria concentrated within 30 μm of the adhesive plaque were mostly (75–100%) dead, as indicated by positive propidium iodide staining, while bacteria beyond 50 μm of the antennules were a more evenly dispersed mixture of live and dead bacteria (Figs 1D, 2A–C, 3A,B,D and 4). In the other half of cases, there was no clear patterning and a mixture of live and dead bacteria were present throughout the interface (Fig. 2D). Occasionally, bacteria surrounding the cyprid adhesive plaque were all dead on one side of the disc and all live on the opposite side. The material was often observed in both of these regions near the adhesive plaque and amidst the developing cuticle, independent of bacteria. Thus, there was no correlation between bacterial viability and the presence of the patchy material.

Protein staining

The interfacial material of newly metamorphosed, stage 6 juveniles stained positively for general protein (SYPRO Ruby 41/41 barnacles; Table 1, Fig. 7; Movie 1, Fig. S3A,C,D) and for phosphoproteins (Pro-Q Diamond, 35/36 barnacles; Table 1; Movie 1, Fig. S3A,B,D). SYPRO Ruby stained large expanses of the material, and revealed that specific regions between adjacent bands of cuticle contain proteins (Fig. 7; Movie 1, Fig. S3A,C,D), which was not evident with the other stains including Pro-Q Diamond. The general protein staining filling the space between the separated cuticle was more expansive at the surface and confined at the cuticle origin on the basis (Movie 1). Pro-Q Diamond staining was evident in the cyprid adhesive plaque (Fig. 7A,C, 8; Movie 1, Fig. S3A,B,D) and the patchy material (Fig. 8; Fig. S3A,B,D). Unstained barnacles showed no autofluorescent material with the excitation and emission settings for either protein stain (Fig. 7E,F).

ROS staining

We examined five live post-metamorphic day 3–5 juveniles using the CellROX orange reagent, which fluoresces when oxidized, and the nucleic acid stain Hoechst 34222 (Fig. 9). CellROX orange showed positive staining in three regions: amidst cuticle bands near the edge of the basis (Fig. 9), the patchy material (Fig. 9C), and within a capillary (Fig. 9D). While the patchy material is often less expansive in day 3–5 juveniles than it is in newly metamorphosed juveniles (stage 6), it was observed with positive CellROX orange staining in the cuticle-associated regions, where the material was

Journal of Experimental Biology (2017) 220, 194-207 doi:10.1242/jeb.145094

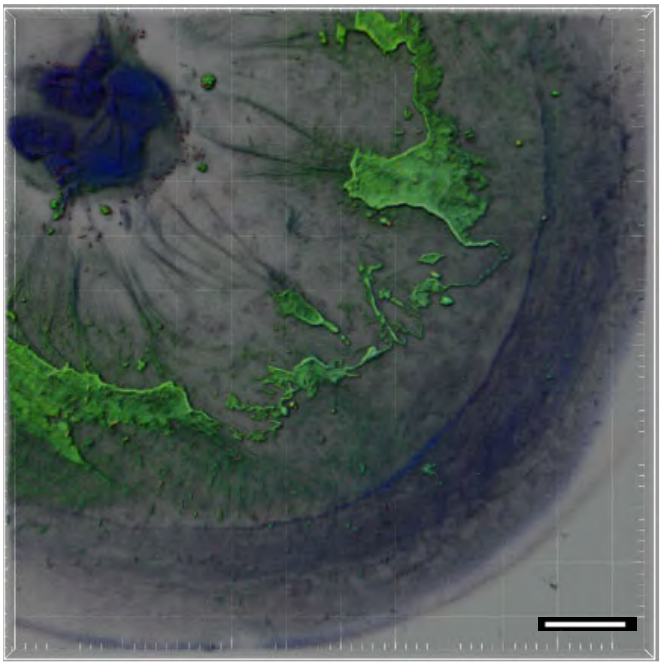

Fig. 4. Three-dimensional rendering showing a relief image with the prominent material within the confocal *Z*-stack. The stage 6 (newly metamorphosed juvenile) barnacle was stained with SYTO 9/propidium iodide for live/dead bacteria. The brightfield image is overlaid to show the edge of the barnacle basis (lower right) in relation to the antennules (upper left in blue), the patchy material (green) with the initial cuticle (green striations) and the adjacent bands of the autofluorescent outer cuticle (blue striations). The red dots around the antennules are dead bacteria and the green dots, interspersed with the patchy material and cuticle, are live bacteria. Scale bar, 30 μm.

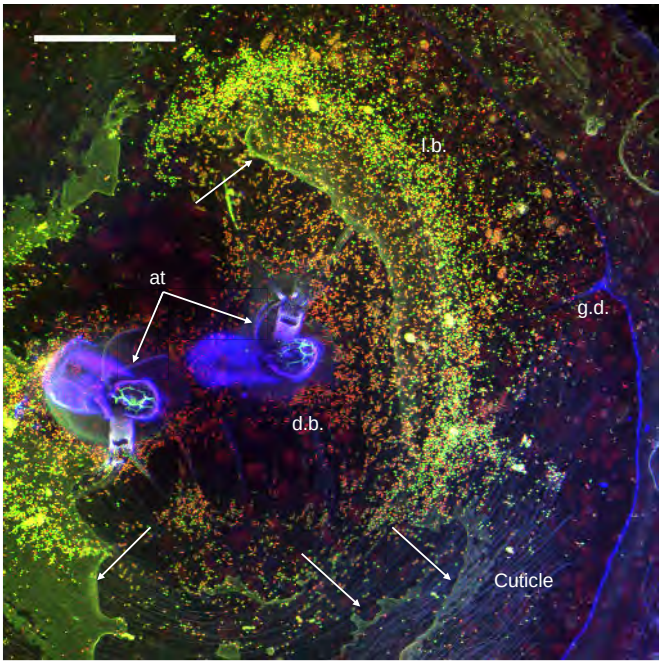

Fig. 5. Confocal microscope image of a day 3–5 juvenile barnacle using a live/dead stain for bacteria. The image shows the antennules (at) anchoring the juvenile and the patchy material (arrows) in green associated with the green/blue autofluorescent bands of cuticle. Dead bacteria (d.b.) in red are prevalent closest to the antennules, while dense live bacteria (l.b.) in green are further away. The first glue duct (g.d.) and capillary ring are autofluorescent blue and were evident closest to the edge of the basis. Scale bar, 50 μm.

observed with other stains (Fig. 9). The nucleic acid dye Hoechst 33342 was used to label bacterial cells in conjunction with ROS staining. Most bacterial cells at the interface stained only with Hoechst 33342, but ones closest to the edge of the basis stained positive with CellROX orange (Fig. 9). Even with the CellROX labeling of some bacteria, this was distinct from its staining of barnacle features at the interface. The cyprid adhesive plaque showed some positive CellROX orange staining (Fig. 9B,E), but controls showed some autofluorescence at these settings in the cyprid adhesive plaque. The autofluorescence was not seen adjacent to the cyprid plaque (Fig. 9E), or in any of the regions of interest associated with the cuticle or where the patchy material appears (Fig. 9F).

DISCUSSION

During the transition from a planktonic to a sessile lifestyle, bacteria between the barnacle basis and substrata were relevant to the dynamics observed at this critical interface. Bacteria associated with the cyprid once it initiated attachment, by releasing cyprid adhesive via antennules. Bacteria seemed to concentrate in specific regions under the barnacle, but died during later stages of settlement and metamorphosis, beginning with those closest to the cyprid adhesive plaque at the antennules. We discuss the implications of the development of the new interfacial material during settlement and metamorphosis and how the observed interactions with bacteria at the interface inform the study of barnacle growth and development.

Our first objective was to characterize the presence and association of bacteria with barnacles at the interface for each stage of settlement, metamorphosis and transition to juvenile. We were surprised to find that the cyprids were free of bacteria prior to settlement. This observation was confirmed with cyprids collected from the field and laboratory cyprids reared without antibiotics. It is likely that *A. amphitrite* in the field reach the cyprid stage quickly and spend only a brief time in the plankton (Rittschof et al., 1984). This may be unique to *A. amphitrite* and other short-lived cyprids as longer-lived barnacle cyprids, such as *Semibalanus (=Balanus) balanoides*, are routinely fouled with bacteria (N. Aldred and A. S. Clare, personal communication). The mechanisms by which cyprids are kept clean of bacteria were not investigated here, but warrant further attention.

As soon as adhesive was released during the early stages of settlement in which cyprids began attachment, bacteria were present, surrounding the antennules first and becoming increasingly abundant throughout the interface as settlement and metamorphosis progressed. While the estimated bacterial density was rather constant until the 1 week old juvenile stage, the distribution was often clumped, surrounding the cyprid plaque and scattered evenly throughout the rest of the area under the basis. The localization of bacteria around the adhesive plaque suggests that bacteria may be attracted to the plaque location via positive chemotaxis. Bacteria surrounding the cyprid adhesive plaque were observed previously (Aldred et al., 2013), which led to the discovery of a lipidaceous barrier to the plaque, covering and perhaps protecting the proteinaceous portion of the adhesive (Gohad et al., 2014), a potential nutrient-rich material for bacteria. By stage 6, the newly metamorphosed juvenile, bacteria were abundant and showed two patterns of viability. In about half of the barnacles at this stage (N=38), bacteria closest to the cyprid adhesive plaque were all dead and bacteria elsewhere had mixed viability. In the other half, bacteria were mixed, live and dead,

Journal of Experimental Biology (2017) 220, 194-207 doi:10.1242/jeb.145094

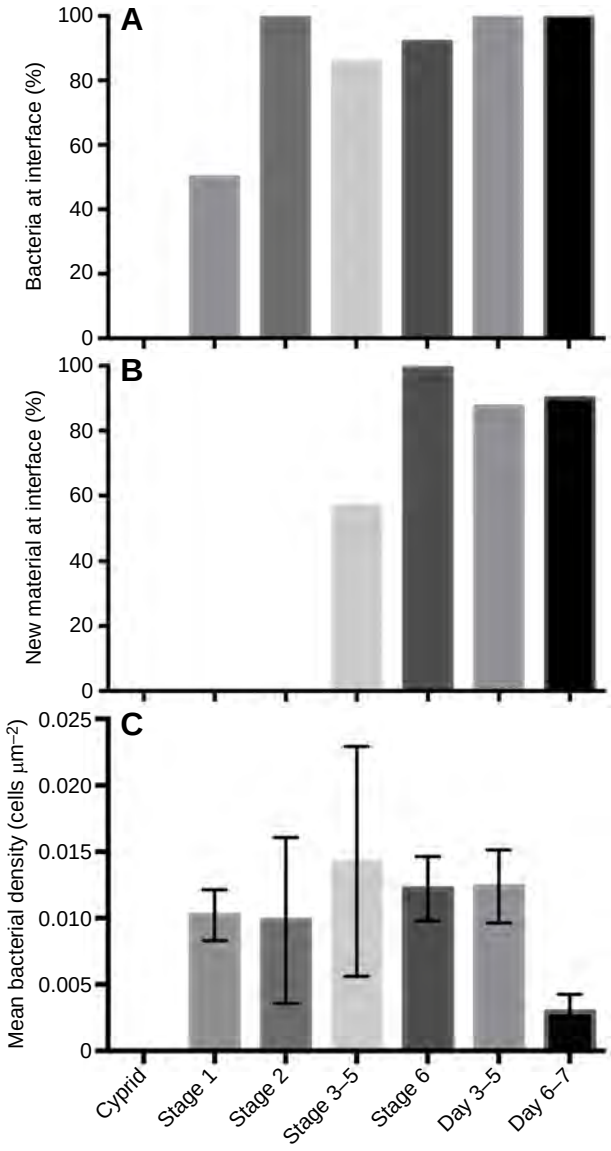

Fig. 6. Occurrence of bacteria and new material to the interface by stage of transition from cyprid to juvenile. (A) Percentage of individual barnacles showing bacteria at the interface. (B) Percentage presence of new material at the interface. (C) Mean bacterial density. Error bars represent s.e.m. Stages were before (cyprid), during (stage 1–6) and after (day 3–5 and day 6–7) settlement and metamorphosis. For bacteria presence: cyprid, *N*=8; stage 1, *N*=6; stage 2, *N*=4; stages 3–5, *N*=14; stage 6, *N*=76; day 3–5, *N*=23; day 6–7, *N*=10. For the new material: cyprid, *N*=8; stage 1, *N*=6; stage 2, *N*=4; stages 3–5, *N*=14; stage 6, *N*=153; day 3–5, *N*=16; day 6–7, *N*=10. For bacterial density: cyprid, *N*=3; stage 1, *N*=3; stage 2, *N*=3; stages 3–5, *N*=3; stage 6, *N*=3; day 3–5, *N*=4; day 6–7, *N*=2. Total count of 0.5–3 μm dots in one plane of the SYTO 9 channel divided by total area in field of view.

without clear patterning. Regardless of the patterning, the period of development at the completion of settlement and metamorphosis was clearly a time of very high mortality of bacteria under the barnacle.

To explain the observation of dead bacteria, we first suspected that the abundance of oxygen might be an issue under the barnacles, as the basis in contact with the substratum eventually becomes a flat surface, presumably rendering the interface uninhabitable by aerobic bacteria. While we did not measure available oxygen under the larvae, confocal imaging shows that there is ample space at the interface even when the larvae are fully metamorphosed: day 3–5, 6.4–34.5 μm; and day 6–7, 11–14 μm. At this critical point for bacterial viability (associated with stage 6 barnacles), only the cyprid antennules embedded in the adhesive plaque and the first rings of cuticle and associated material are in contact with the substratum, leaving space elsewhere. While it is possible that the observed bacteria may all be capable of anaerobic respiration, a limitation of oxygen for the bacteria in this space is unlikely, but not impossible.

A plausible explanation for the bacterial mortality observed is the presence of antimicrobial agents at the interface. We observed positive staining for oxidative chemistries associated with the developing cuticle, which may account for the observed cytotoxicity of bacteria. The generation of ROS, or free radicals, can explain the observed mortality of bacterial populations (Bandyopadhyay et al., 1999; Cabiscol et al., 2000; Fang, 2004) under the barnacle. The data show that oxidative chemistries were present in several interface features including the cuticle, the patchy material and within a capillary, a feature that delivers one type of barnacle cement secretion to the interface (Burden et al., 2012). The bacterial staining showed that the ROS was largely distinct from the bacteria and from features of the barnacle. We hypothesize that these ROS at the cuticle layers also contribute to oxidative crosslinking (Okay et al., 1995; Dijkgraaf et al., 2003; Lattuada et al., 2013), as seen in other crustaceans (Willis, 1999; Glazer et al., 2013), and are critical to cuticle development and hardening, as seen in insects (Hopkins and Kramer, 1992; Suderman et al., 2006; Andersen, 2010). Further work is needed to define the specific ROS present and show the extent of their presence during development as only post-metamorphic juveniles were examined. Additional investigation is needed to determine whether ROS is one of the mechanisms by which these cyprids are kept free of bacteria.

Because of their role in crosslinking and antimicrobial activity, oxidative chemistries, including ROS, are commonly delivered to wound sites (Winston et al., 1996; Kanost et al., 2004; Labreuche et al., 2006; Cerenius et al., 2010) in many animals, including crustaceans such as crabs and shrimp (Bell and Smith, 1993; Campa-Córdova et al., 2002). It is possible that the developing cuticle undergoes tearing, especially in later stages of metamorphosis, concurrent with substantial changes to the barnacle shape. Consistent with the suggestion of oxidative crosslinking at the developing interface, recent studies of adult barnacle interfaces using *in situ* cyclic voltammetry have revealed electrochemical behavior consistent with the presence of redox active compounds (Golden et al., 2016), as well as spectroscopic evidence for the presence of phenolic compounds in interfacial barnacle fluids (Burden et al., 2012). Quinone tanning can be driven by free radicals or enzymes and mediates crosslinking in diverse systems and contexts, including sclerotized insect cuticle and mussel byssal threads (Korytowski et al., 1987; Waite, 1995; Suderman et al., 2006; Yang et al., 2014). Surprisingly, antimicrobial properties of barnacle secretions have not been deeply explored, even after the identification of a barnacle cement protein with homology to the antibacterial enzyme lysozyme (Kamino and Shizuri, 1998).

Our second major finding was the presence of a novel interfacial material under larvae midway through settlement and metamorphosis until the 1 week old post-metamorphic juvenile stage. The material, present in nearly all newly metamorphosed juveniles, consisted of irregularly shaped patches between and surrounding the cuticle folds. The irregularity of the material suggested it was originally released as fluid and coagulated at semi-

Journal of Experimental Biology (2017) 220, 194-207 doi:10.1242/jeb.145094

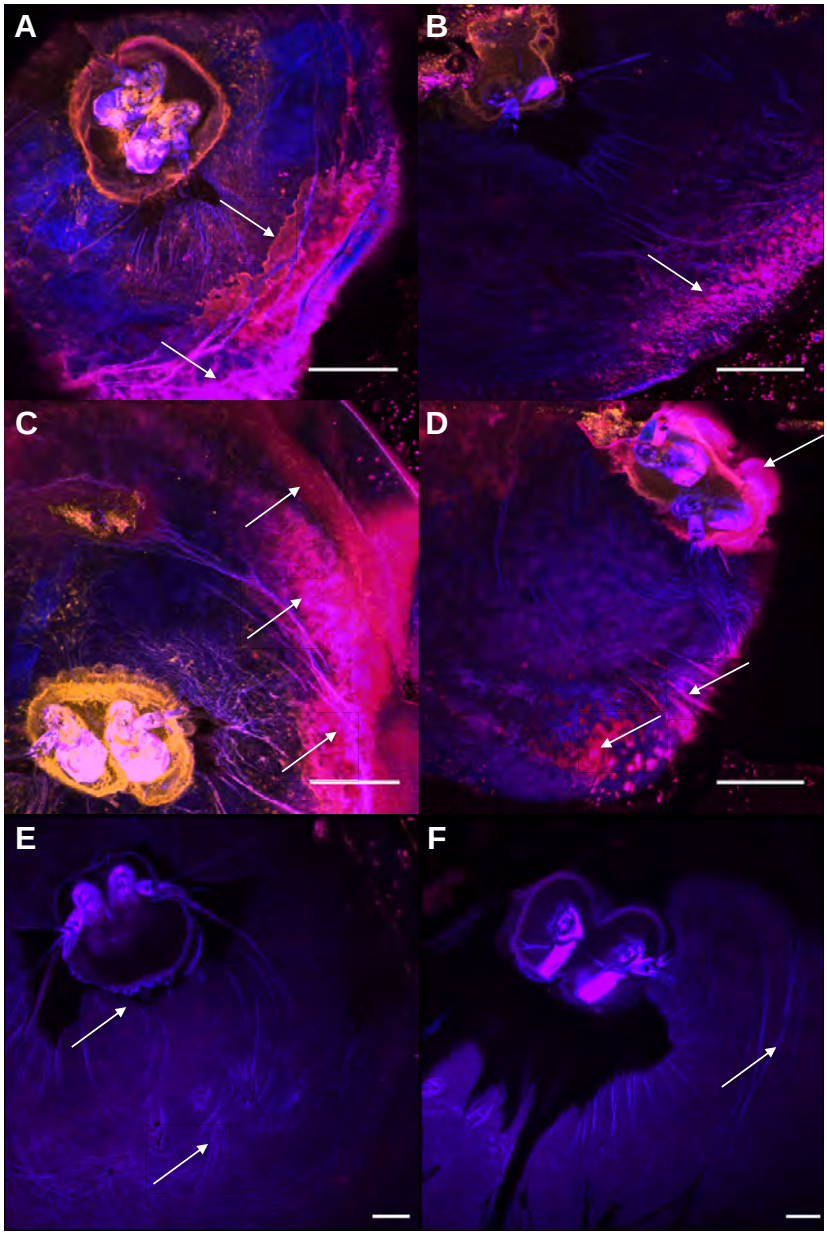

Fig. 7. Confocal microscope images of four newly metamorphosed juvenile (stage 6) barnacles stained with SYPRO Ruby for general protein (red/pink). Because of the imaging conditions (excitation 405 nm), there is overlap for the autofluorescence (blue) and the emission for SYPRO Ruby (red), yielding some pink regions. Regions with only autofluorescence appear blue and are the antennules and tissue of the barnacle basis. Proteinaceous material is dark pink associated with the antennules. Patchy new material (arrows) stains pink (A,B) as does space between bands of cuticle, as indicated by arrows (A–D). The yellow within the antennular plaque is residual stain from Pro-Q Diamond, which was done first. Control images were unstained and imaged with the same excitation/emission settings for both protein stains (SYPRO Ruby and Pro-Q Diamond) (E,F). Controls show no signal, consistent with the protein staining, and only show autofluorescence from 405 nm excitation. Arrows on control images indicate typical regions where protein staining was positive in treated samples (E,F). Scale bars: A–D, 50 μm; E,F, 20 μm.

irregular locations, but never filled the entirety of the area of the basis. The patchy material spanned the depth of the interface, demonstrating it physically contacts both the barnacle basis and the substratum. While the patchy material was first observed with the nucleic acid stains, the protein stains suggest the material was mainly proteinaceous and at least some proteins were phosphorylated. Cyprid adhesive and adult glues contain a large fraction of protein (Kamino and Shizuri, 1998; Urushida et al., 2007; He et al., 2013; Gohad et al., 2014). Phosphoprotein was of particular interest as it was found in the cyprid adhesive plaque (Gohad et al., 2014) and is a critical component of other marine adhesives such as mussel (Waite and Qin, 2001; Flammang et al., 2009). Additionally, phosphoproteins are important to the development of extracellular matrices and the transition to calcification (Borbas et al., 1991; Arias et al., 1993; George et al., 1993; Fernández et al., 2002; Johnstone et al., 2015a). Barnacle baseplate and shell biomineralization involve an initial organic matrix in which calcite crystals form (Fernández et al., 2002; Mori et al., 2007; Lewis et al., 2014), with the potential for involvement of calcite-carrying hemocytes, as seen in oyster calcification (Mount et al., 2004; Zhang et al., 2013; Johnstone et al., 2015; Li et al., 2016). Estimates of barnacle hemocyte concentrations are 1.7×10^2 cells μl^{-1} hemolymph, mostly composed of hyaline cells and some semigranular cells (Waite and Walker, 1988; Dickinson et al., 2009). Our knowledge of barnacle hemocyte function is limited, but they may phagocytose bacteria (Waite and Walker, 1988) and lyse upon contact with air, releasing the crosslinking enzyme transglutaminase (Martin et al., 1991; Dickinson et al., 2009). Based on staining observations, the material occurring at the interface of newly metamorphosed juveniles contains a mixture of proteins, phosphoproteins and nucleic acids. While the finding that the patchy material stained for nucleic acids was unexpected, this may be due to release of nucleic acids from hemocytes upon delivery to the interface and apoptotic events during tissue morphogenesis and development. Further work is needed to explore the nucleic acid content of the patchy material and the

Journal of Experimental Biology (2017) 220, 194-207 doi:10.1242/jeb.145094

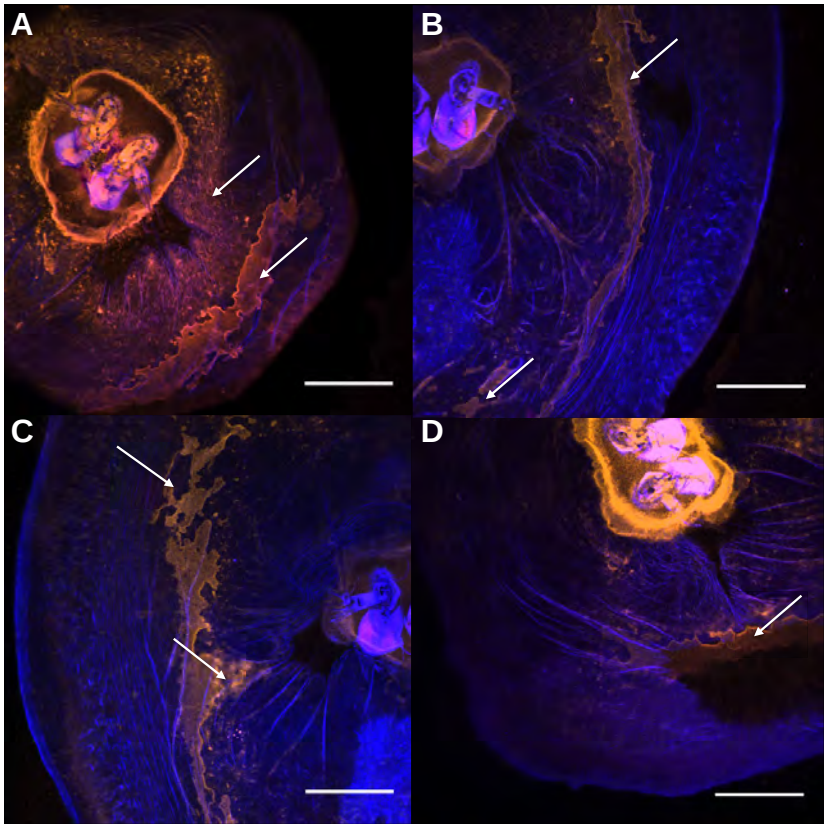

Fig. 8. Confocal microscope images of stage 6 barnacles stained with Pro-Q Diamond for phosphoproteins (orange). Autofluorescence, with 405 nm excitation, shows antennules (blue/purple) surrounded by the adhesive plaque (orange). Patchy material stains orange amidst cuticle striations (blue) (A–D). Arrows show the interfacial material staining for phosphoprotein. Scale bars, 50 μm.

role of hemocytes, to elucidate aspects of barnacle interface development and growth.

The patchy material is clearly not extracellular polymeric substance (EPS) because many bacteria-rich areas are not stained. The material could originate via two potential mechanisms: either the substance is secreted to the interface via defined secretory orifices or it is leaked as a result of physical damage to tissues underlying the cuticle. If the material were released from a duct system, it would be more regular in deposition patterning than what was observed. The two known secretion routes of cement to the interface in barnacles are movement of the cyprid adhesive from the cement glands through the antennules (Yule and Walker, 1984) and via a network of capillaries and ducts in the adult that deliver spots of cement secretion (Burden et al., 2012), 40 days after metamorphosis (Walker, 1973). The patchy material we found under juveniles is distinct from both of these. It is spatially distinct from the cyprid adhesive plaque, which originates in stage 1 and has a clear boundary (Gohad et al., 2014) separating the plaque from this material. The second route of secretion is not active until the adult cement system matures (Yule and Walker, 1984). The first one or two sets of capillaries and ducts were observed after stage 6, in day 3–5 and day 6–7 juveniles, indicating that the establishment of the duct network begins earlier in *A. amphitrite* than it does in *S. balanoides*. In *A. amphitrite*, the patchy material appears temporally and spatially distinct from the development and location of the capillaries and ducts at the interface. In post-metamorphic juveniles, capillaries occur closer to the edge of the basis, whereas the interfacial material occurs midway between the cyprid adhesive plaque from the antennules and the capillaries and ducts at the edge of the basis. These arguments discount the possibility that the material originates from previously described secretory orifices and mechanisms.

Instead, the evidence strongly suggests that the material leaks through the developing cuticle, during the late stages of metamorphosis, while it undergoes organization and expansion. The development of new cuticle during growth is well characterized, especially in terms of the timing of the formation of multiple layers in relation to growth and molting (Bocquet-Vedrine, 1965; Bourget and Crisp, 1975; Anderson, 1994). The cuticle layers add flexibility to the exoskeleton, as the growth front extends (Bocquet-Vedrine, 1965; Anderson, 1994; Burden et al., 2014). The new underlying layer of folded cuticle develops and eventually replaces the interfacial layer, which stretches and tears (Bourget and Crisp, 1975; Anderson, 1994). The process of stretching and tearing of epicuticle may include tearing of underlying tissue layers, potentially resulting in the loss of fluids to the interface. Recent evidence suggests interfacial fluids are associated with cuticle expansion at the growth front (Burden et al., 2012).

An additional hypothesis is that the material is secreted from stores within the cuticle layers upon activation by molecules that recognize microbial patterns. Pattern recognition proteins are ubiquitous in crustacean innate immune systems (Medzhitov and Janeway, 2000; Vasta et al., 2007; Vazquez et al., 2009; Wang and Wang, 2013) and often activate coagulation of proteinaceous material with antimicrobial consequences (Martin et al., 1991; Jiravanichpaisal et al., 2006; Schmidt et al., 2010; Loof et al., 2011). The origin of the fluids associated with cuticle expansion remains unanswered and requires further attention.

After metamorphosis, the surface area parallel to the substratum increases substantially from two small points of the cyprid antennules to a larger circular basis. The patchy material physically connects the barnacle and substratum at this interface, and likely provides additional attachment support. Although

Journal of Experimental Biology (2017) 220, 194-207 doi:10.1242/jeb.145094

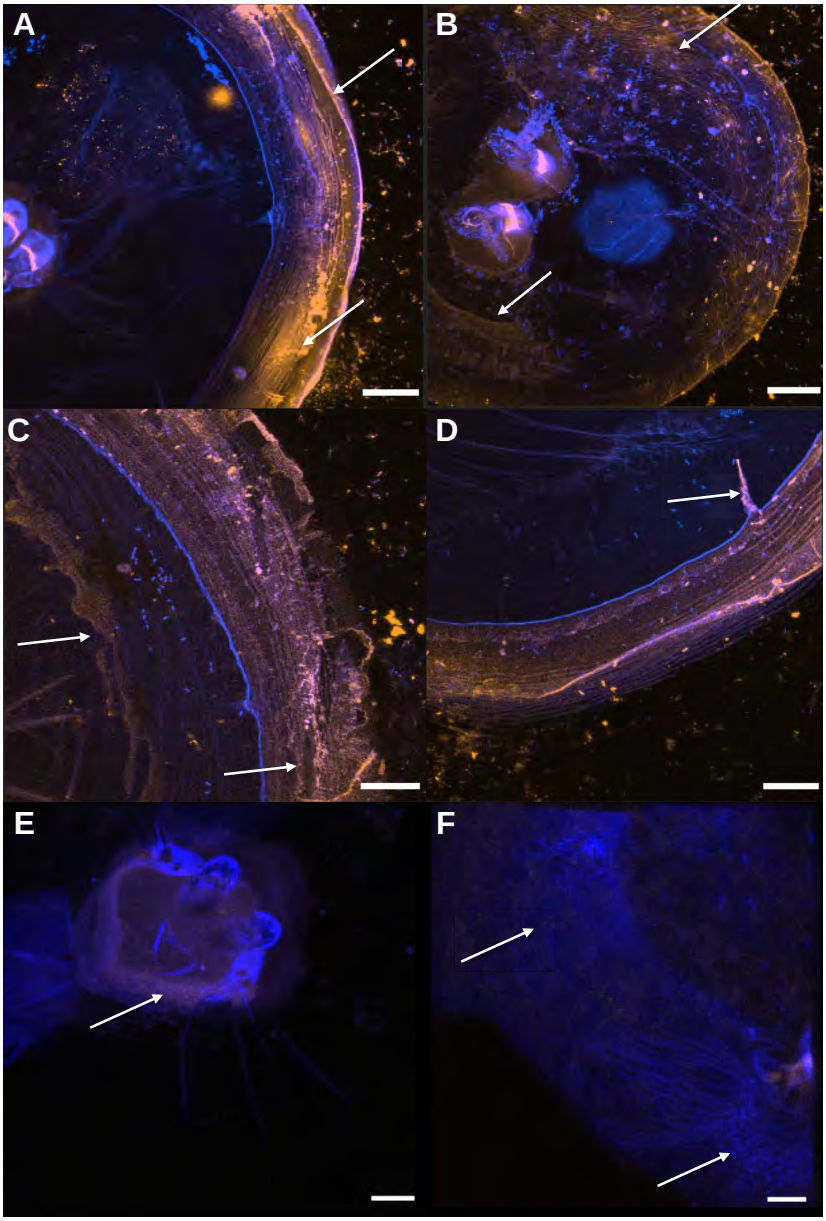

Fig. 9. Confocal images of unfixed post-metamorphic (day 3–5) juvenile barnacles stained with CellROX orange for oxidative chemistry and Hoechst 34222 for nucleic acids. Live juvenile barnacles were used. (A) Positive staining amidst banded cuticle (orange bands) and bacteria (blue dots) is present at the interface. Arrows indicate ROS staining in cuticle bands. Scale bar, 40 μm. (B) Positive staining is again seen amidst cuticle near the edge and the patchy material (arrow); antennules had autofluorescence at the settings for CellROX orange. Scale bar, 40 μm. (C) Positive staining of patchy material (arrow) and outer cuticle bands just after a capillary is shown. Scale bar, 20 μm. (D) Positive staining is present along the outer cuticle (orange, banded pattern) and within a capillary (arrow). Scale bar, 20 μm. (E) Control image with unstained barnacle with the excitation/emission settings for CellROX orange and Hoechst 34222, showing the antennules embedded in the adhesive plaque in blue and some degree of autofluorescence in orange within the plaque (arrow). Scale bar, 15 μm. (F) Control image with unstained barnacle showing only blue autofluorescence of the cuticle from the 405 nm excitation and no orange where it was seen amidst cuticle (arrows) in stained samples. Scale bar, 15 μm.

attachment strength was not measured here, it has been shown that within the first 2 weeks following metamorphosis, juvenile *S. balanoides* adhere more strongly than the force of the cyprid adhesive alone (Yule and Walker, 1984). Yule and Walker (1984) removed the juvenile and stained the substratum and basis with Bromophenol Blue, revealing a proteinaceous material on juvenile bases that was suspected to originate from the hypodermis. Their findings support our observations as they report the area of the juvenile cement was of variable symmetry and covered a large portion of the basis (Yule and Walker, 1984).

In summary, we observed that proteinaceous material is deposited concurrent with cuticle development and patches of material fill the interface between the barnacle basis and the substratum. In these stages of development, expansion of a robust adhesive interface is critical for barnacle survival. Therefore, we postulate that cuticle tearing is associated with the deposition and expansion of a cement-like material and hypothesize that this material is a candidate for mediating attachment. Furthermore, two previous studies demonstrated an increase in adhesion mid-metamorphosis and immediately following metamorphosis (Yule and Walker, 1984; Zardus et al., 2008), corresponding with the stage at which this material was observed. The previously observed difference in adhesion of barnacles mid-metamorphosis on biofilm-coated surfaces (Zardus et al., 2008) may indicate that the process of killing bacteria at the interface is important to cement curing mechanisms. One barnacle glue curing mechanism for which there is evidence is proteolytic cascades similar to blood coagulation (Dickinson et al., 2009). The possibility that barnacle adhesive fluids have abilities associated with wound healing, combined with a dynamic cuticle from which the observed fluids may be released, is an interesting avenue of comparative biology research.

Arthropod cuticle is not solely a physical barrier to the environment but can contribute to critical processes such as immune responses and cross-linking for cuticle hardening and calcification of exoskeleton (Ashida and Brey, 1995; Sugumaran and Nelson, 1998; Adachi et al., 2005; Suderman et al., 2006; Glazer et al., 2013). In crustaceans, cuticle tearing leaks hemolymph and releases proteins, which coagulate sealing the wound and

preventing infection (Iwanaga et al., 1998; Li et al., 2002; Jiravanichpaisal et al., 2006). Crustacean circulatory fluids contain different compositions of proteins and hormones depending on the stage of molting (Vacca and Fingerman, 1983; Engel and Brouwer, 1987; Terwilliger, 1999; Engel et al., 2001), further underscoring the importance of considering timing when studying these materials. Like vertebrate bodily fluids (Davie and Ratnoff, 1964; Furie and Furie, 1988), hemolymph also contains proteins involved in coagulation, activated upon wounding (Nagai and Kawabata, 2000; Li et al., 2002; Theopold et al., 2002, 2004; Dickinson et al., 2009). The two functions of stopping the loss of bodily fluid and preventing infection are routinely linked; most mechanisms for coagulation provide antimicrobial activity (Iwanaga et al., 1998; Li et al., 2002; Cerenius and Söderhäll, 2004; Theopold et al., 2004). Multifunctional cytotoxic byproducts, including quinones from protein crosslinking and ROS (Bandyopadhyay et al., 1999; Nappi and Ottaviani, 2000; Abele and Puntarulo, 2004; Apel and Hirt, 2004; Nappi and Christensen, 2005) also act as bacteriocides. The findings presented here inform crustacean larval development during the critical time of settlement and metamorphosis and provide insight into potential attachment mechanisms that may be relevant throughout juvenile and adult barnacle growth.

Acknowledgements
The authors gratefully acknowledge Dr J. S. Maki at Marquette University for his assistance estimating bacteria load from seawater samples and the Duke Light Microscopy Facility for their expertise and resources.

Competing interests
The authors declare no competing or financial interests.

Author contributions
The experimental work, image acquisition, processing, analysis and writing of the results were performed by T.E.-B. and led by D.R. Support of experimental concepts and manuscript preparation was received from K.W., A.S.M. and C.S. Rearing of barnacle larvae and technical support and expertise were from B.O. Confocal training and support was from N.G., A.S.M. and C.S.

Funding
This work was funded by the Office of Naval Research [N000141210365 and N000141410336 at Duke to D.R., T.E.-B. and B.O.; N000141110183 at Clemson to A.M. and N.G.; and N0001415WX01915 at NRL to K.W. and C.S.], Naval Research Enterprise Internship Program (to T.E.-B. for work in the lab of K.W.), Oak Foundation graduate enhancement funding (to T.E.-B. to work in the lab of A.S.M.) and Naval Research Laboratory base funding.

Data availability
Additional confocal data are available upon request from the corresponding author.

Supplementary information
Supplementary information available online at
http://jeb.biologists.org/lookup/doi/10.1242/jeb.145094.supplemental

References
Abele, D. and Puntarulo, S. (2004). Formation of reactive species and induction of antioxidant defence systems in polar and temperate marine invertebrates and fish. *Comp. Biochem. Physiol. A Mol. Interg. Physiol.* **138**, 405-415.
Adachi, K., Endo, H., Watanabe, T., Nishioka, T. and Hirata, T. (2005). Hemocyanin in the exoskeleton of crustaceans: enzymatic properties and immunolocalization. *Pigment Cell Res.* **18**, 136-143.
Aldred, N. and Clare, A. S. (2008). The adhesive strategies of cyprids and development of barnacle-resistant marine coatings. *Biofouling* **24**, 37-41.
Aldred, N., Gohad, N. V., Petrone, L., Orihuela, B., Liedberg, B., Ederth, T., Mount, A., Rittschof, D. and Clare, A. S. (2013). Confocal microscopy-based goniometry of barnacle cyprid permanent adhesive. *J. Exp. Biol.* **216**, 1969-1972.
Andersen, S. O. (2010). Insect cuticular sclerotization: a review. *Insect Biochem. Mol. Biol.* **40**, 166-178.
Anderson, D. T. (1994). Growth. In *Barnacles: Structure, Function, Development and Evolution*, pp. 247-286. London: Chapman & Hall.
Apel, K. and Hirt, H. (2004). Reactive oxygen species: metabolism, oxidative stress, and signal transduction. *Annu. Rev. Plant Biol.* **55**, 373-399.
Arias, J. L., Fink, D. J., Xiao, S.-Q., Heuer, A. H. and Caplan, A. I. (1993). Biomineralization and eggshells: cell-mediated acellular compartments of mineralized extracellular matrix. *Int. Rev. Cytol.* **145**, 217-250.
Ashida, M. and Brey, P. T. (1995). Role of the integument in insect defense: pro-phenol oxidase cascade in the cuticular matrix. *Proc. Natl. Acad. Sci. USA* **92**, 10698-10702.
Bacchetti De Gregoris, T., Khandeparker, L., Anil, A. C., Mesbahi, E., Burgess, J. G. and Clare, A. S. (2012). Characterisation of the bacteria associated with barnacle, *Balanus amphitrite*, shell and their role in gregarious settlement of cypris larvae. *J. Exp. Mar. Biol. Ecol.* **413**, 7-12.
Bandyopadhyay, U., Das, D. and Banerjee, R. K. (1999). Reactive oxygen species: oxidative damage and pathogenesis. *Curr. Sci.* **77**, 658-666.
Barnes, H. and Blackstock, J. (1974). The biochemical composition of the cement of a pedunculate cirripede. *J. Exp. Mar. Biol. Ecol.* **16**, 87-91.
Bell, K. L. and Smith, V. J. (1993). In vitro superoxide production by hyaline cells of the shore crab *Carcinus maenas* (L.). *Dev. Comp. Immunol.* **17**, 211-219.
Bocquet-Vedrine, J. (1965). Etude du tegument et da la mue chez le cirripede opercule *Elminius modestus* Darwin. *Arch. Zool. Exp. Gen.* **105**, 30-76bour.
Borbas, J. E., Wheeler, A. P. and Sikes, C. S. (1991). Molluscan shell matrix phosphoproteins: Correlation of degree of phosphorylation to shell mineral microstructure and to in vitro regulation of mineralization. *J. Exp. Zool.* **258**, 1-13.
Boulos, L., Prévost, M., Barbeau, B., Coallier, J. and Desjardins, R. (1999). LIVE/DEAD® BacLight™: application of a new rapid staining method for direct enumeration of viable and total bacteria in drinking water. *J. Microbiol. Methods* **37**, 77-86.
Bourget, E. and Crisp, D. J. (1975). An analysis of the growth bands and ridges of barnacle shell plates. *J. Mar. Biol. Assoc. UK* **55**, 439-461.
Burden, D. K., Barlow, D. E., Spillmann, C. M., Orihuela, B., Rittschof, D., Everett, R. K. and Wahl, K. J. (2012). Barnacle *Balanus amphitrite* adheres by a stepwise cementing process. *Langmuir* **28**, 13364-13372.
Burden, D. K., Spillmann, C. M., Everett, R. K., Barlow, D. E., Orihuela, B., Deschamps, J. R., Fears,, K. P., Rittschof, D. and Wahl, K. J. (2014). Growth and development of the barnacle *Balanus amphitrite*: time- and spatially-resolved structure and chemistry of the base plate. *Biofouling* **30**, 799-812.
Cabiscol, E., Tamarit, J. and Ros, J. (2000). Oxidative stress in bacteria and protein damage by reactive oxygen species. *Int. Microbiol.* **3**, 3-8.
Callow, M. E. and Callow, J. A. (2002). Marine biofouling: a sticky problem. *Biologist* **49**, 10-14.
Campa-Córdova, A. I., Hernández-Saavedra, N. Y., De Phillipis, R. and Ascencio, F. (2002). Generation of superoxide anion and SOD activity in haemocytes and muscle of American white shrimp (*Litopenaeus vannamei*) as a response to *β*-glucan and sulphated polysaccharide. *Fish Shellfish Immunol.* **12**, 353-366.
Cerenius, L. and Söderhäll, K. (2004). The prophenoloxidase-activating system in invertebrates. *Immunol. Rev.* **198**, 116-126.
Cerenius, L., Jiravanichpaisal, P., Liu, H.-p. and Söderhäll, I. (2010). Crustacean immunity. *Adv. Exp. Med. Biol.* **708**, 239-259.
Crisp, D. J. (1955). The behaviour of barnacle cyprids in relation to water movement over a surface. *J. Exp. Biol.* **32**, 569-590.
Crisp, D. J. (1960). Mobility of barnacles. *Nature* **187**, 1048-1049.
Crisp, D. J. (1969). Studies of barnacle hatching substance. *Comp. Biochem. Physiol.* **30**, 1037-1048.
Crisp, D. J. and Bourget, E. (1985). Growth in Barnacles. In *Advances in Marine Biology*, Vol. 22 (ed. J. H. S. Blaxter and F. S. Russel), pp. 199-244. incollection, London: Academic Press Inc.
Crisp, D. J. and Meadows, P. S. (1963). Adsorbed layers: the stimulus to settlement in barnacles. *Proc. R. Soc. B* **158**, 364-387.
Davie, E. W. and Ratnoff, O. D. (1964). Waterfall sequence for intrinsic blood clotting. *Science* **145**, 1310-1312.
Desjardins, R., Boulos, L. Barbeau, B. (1999). LIVE/DEAD ® Bac Light E: application of a new rapid staining method for direct enumeration of viable and total bacteria in drinking water. *J. Microbiol. Meth.* **37**, 77-86.
Dickinson, G. H., Vega, I. E., Wahl, K. J., Orihuela, B., Beyley, V., Rodriguez, E. N., Everett, R. K., Bonaventura, J. and Rittschof, D. (2009). Barnacle cement: a polymerization model based on evolutionary concepts. *J. Exp. Biol.* **212**, 3499-3510.
Dijkgraaf, L. C., Zardeneta, G., Cordewener, F. W., Liem, R. S. B., Schmitz, J. P., de Bont, L. G. M. and Milam, S. B. (2003). Crosslinking of fibrinogen and fibronectin by free radicals: a possible initial step in adhesion formation in osteoarthritis of the temporomandibular joint. *J. Oral Maxillofac. Surg.* **61**, 101-111.
Dobretsov, S. and Thomason, J. C. (2011). The development of marine biofilms on two commercial non-biocidal coatings: a comparison between silicone and fluoropolymer technologies. *Biofouling* **27**, 869-880.
Dobretsov, S., Dahms, H.-U. and Qian, P. I.-Y. (2006). Inhibition of biofouling by marine microorganisms and their metabolites. *Biofouling* **22**, 43-54.
Dreanno, C., Kirby, R. R. and Clare, A. S. (2006a). Locating the barnacle settlement pheromone: spatial and ontogenetic expression of the settlement-

inducing protein complex of *Balanus amphitrite*. *Proc. R. Soc. B Biol. Sci.* **273**, 2721-2728.
Dreanno, C., Matsumura, K., Dohmae, N., Takio, K., Hirota, H., Kirby, R. R. and Clare, A. S. (2006b). An alpha2-macroglobulin-like protein is the cue to gregarious settlement of the barnacle *Balanus amphitrite*. *Proc. Natl Acad. Sci. USA* **103**, 14396-14401.
Engel, D. W. and Brouwer, M. (1987). Metal regulation and molting in the blue crab, *Callinectes sapidus*: copper, zinc and metallothionein. *Biol. Bull.* **173**, 239-251.
Engel, D. W., Brouwer, M. and Mercaldo-Allen, R. (2001). Effects of molting and environmental factors on trace metal body-burdens and hemocyanin concentrations in the American lobster, *Homarus americanus*. *Mar. Environ. Res.* **52**, 257-269.
Fang, F. C. (2004). Antimicrobial reactive oxygen and nitrogen species: concepts and controversies. *Nat. Rev. Microbiol.* **2**, 820-832.
Fernández, M. S., Vergara, I., Oyarzun, A. and Arias, J. L. (2002). Extracellular matrix molecules involved in barnacle shell mineralization. *Mater. Res. Soc. Symp. Proc.* **724**, 3-9.
Flammang, P., Lambert, A., Bailly, P. and Hennebert, E. (2009). Polyphosphoprotein-containing marine adhesives. *J. Adhes.* **85**, 447-464.
Furie, B. and Furie, B. C. (1988). The molecular basis of blood coagulation. *Cell* **53**, 505-518.
George, A., Sabsay, B., Simonian, P. A. L. and Veis, A. (1993). Characterization of a novel dentin matrix acidic phosphoprotein: Implications for induction of biomineralization. *J. Biol. Chem.* **268**, 12624-12630.
Glazer, L., Tom, M., Weil, S., Roth, Z., Khalaila, I., Mittelman, B. and Sagi, A. (2013). Hemocyanin with phenoloxidase activity in the chitin matrix of the crayfish gastrolith. *J. Exp. Biol.* **216**, 1898-1904.
Gohad, N. V., Dickinson, G. H., Orihuela, B., Rittschof, D. and Mount, A. S. (2009). Visualization of putative ion-transporting epithelia in Amphibalanus amphitrite using correlative microscopy: Potential function in osmoregulation and biomineralization. *J. Exp. Mar. Biol. Ecol.* **380**, 88-98.
Gohad, N. V., Aldred, N., Orihuela, B., Clare, A. S., Rittschof, D. and Mount, A. S. (2012). Observations on the settlement and cementation of barnacle (Balanus amphitrite) cyprid larvae after artificial exposure to noradrenaline and the locations of adrenergic-like receptors. *J. Exp. Mar. Biol. Ecol.* **416**, 153-161.
Gohad, N. V., Aldred, N., Hartshorn, C. M., Jong Lee, Y., Cicerone, M. T., Orihuela, B., Clare, A. S., Rittschof, D. and Mount, A. S. (2014). Synergistic roles for lipids and proteins in the permanent adhesive of barnacle larvae. *Nat. Commun.* **5**, 4414.
Golden, J. P., Burden, D. K., Fears, K. P., Barlow, D. E., So, C. R., Burns, J., Miltenberg, B., Orihuela, B., Rittshof, D., Spillmann, C. M. et al. (2016). Imaging active surface processes in barnacle adhesive interfaces. *Langmuir* **32**, 541-550.
Hadfield, M. G. (1986). Settlement and recruitment of marine invertebrates: a perspective and some proposals. *Bull. Mar. Sci.* **39**, 418-425.
Hadfield, M. G. (2011). Biofilms and marine invertebrate larvae: what bacteria produce that larvae use to choose settlement sites. *Ann. Rev. Mar. Sci.* **3**, 453-470.
He, L. S., Zhang, G. and Qian, P.-Y. (2013). Characterization of two 20kDa-cement protein (cp20k) homologues in *Amphibalanus amphitrite*. *PLoS ONE* **8**, e64130.
Hillman, R. E. and Nace, P. F. (1970). Histochemistry of barnacle cyprid adhesive formation. In *Adhesion in Biological Systems* (ed. R. S. Manly), pp. 113-121. New York: Academic Press.
Holm, E. R. (1990). Attachment behavior in the barnacle *Balanus amphitrite amphitrite* (Darwin): genetic and environmental effects. *J. Exp. Mar. Biol. Ecol.* **135**, 85-98.
Holm, E. R. (2012). Barnacles and biofouling. *Integr. Comp. Biol.* **52**, 348-355.
Hopkins, T. L. and Kramer, K. J. (1992). Insect cuticle sclerotization[1]. *Annu. Rev. Entomol* **37**, 273-302.
Iwanaga, S., Kawabata, S.-i. and Muta, T. (1998). New types of clotting factors and defense molecules found in horseshoe crab hemolymph: their structures and functions. *J. Biochem.* **123**, 1-15.
Jiravanichpaisal, P., Lee, B. L. and Söderhäll, K. (2006). Cell-mediated immunity in arthropods: hematopoiesis, coagulation, melanization and opsonization. *Immunobiology* **211**, 213-236.
Johnstone, M. B., Gohad, N. V., Falwell, E. P., Hansen, D. C., Hansen, K. M. and Mount, A. S. (2015). Cellular orchestrated biomineralization of crystalline composites on implant surfaces by the eastern oyster, *Crassostrea virginica* (Gmelin, 1791). *J. Exp. Mar. Biol. Ecol.* **463**, 8-16.
Joseph, A. Q., Jian, L., Clemen, X., Han, S. J., Leader, T. and Dickinson, G. H. (2011). Potential of barnacle cement in dentistry. *Innov. Mag.* **10**, 14-19.
Kamino, K. (2001). Novel barnacle underwater adhesive protein is a charged amino acid-rich protein constituted by a Cys-rich repetitive sequence. *Biochem. J.* **356**, 503-507.
Kamino, K. (2013). Mini-review: barnacle adhesives and adhesion. *Biofouling* **29**, 735-749.
Kamino, K. and Shizuri, Y. (1998). Structure and function of barnacle cement proteins. In *New Developments in Marine Biotechnology* (ed. L. Gal and H. O. Halvorson), pp. 77-80. New York: Plenum Press.
Kamino, K., Odo, S. and Maruyama, T. (1996). Cement proteins of the acorn-barnacle, Megabalanus rosa. *Biol. Bull.* **190**, 403-409.
Kanost, M. R., Jiang, H. and Yu, X.-Q. (2004). Innate immune responses of a lepidopteran insect, *Manduca sexta*. *Immunol. Rev.* **198**, 97-105.
Khandeparker, L. and Anil, A. C. (2011). Role of conspecific cues and sugars in the settlement of cyprids of the barnacle, *Balanus amphitrite*. *J. Zool.* **284**, 206-214.
Khandeparker, L., Anil, A. C. and Raghukumar, S. (2006). Relevance of biofilm bacteria in modulating the larval metamorphosis of Balanus amphitrite. *FEMS Microbiol. Ecol.* **58**, 425-438.
Knight-Jones, E. W. and Crisp, D. J. (1953). Gregariousness in barnacles in relation to the fouling of ships and to anti-fouling research. *Nature* **171**, 1109-1110.
Knight-Jones, E. W. and Stevenson, J. P. (1950). Gregariousness during settlement in the barnacle *Elminius modestus* Darwin. *J. Mar. Biol. Assoc. UK* **29**, 281-297.
Korytowski, W., Sarna, T., Kalyanaraman, B. and Sealy, R. C. (1987). Tyrosinase-catalyzed oxidation of dopa and related catechol (amine)s: a kinetic electron spin resonance investigation using spin-stabilization and spin label oximetry. *Biochim. Biophys. Acta* **924**, 383-392.
Labreuche, Y., Lambert, C., Soudant, P., Boulo, V., Huvet, A. and Nicolas, J.-L. (2006). Cellular and molecular hemocyte responses of the Pacific oyster, *Crassostrea gigas*, following bacterial infection with *Vibrio aestuarianus* strain 01/32. *Microbes Infect.* **8**, 2715-2724.
Lattuada, M., Del Gado, E., Abete, T., de Arcangelis, L., Lazzari, S., Diederich, V., Storti, G. and Morbidelli, M. (2013). Kinetics of free-radical cross-linking polymerization: Comparative experimental and numerical study. *Macromolecules* **46**, 5831-5841.
Lewis, A. C., Burden, D. K., Wahl, K. J. and Everett, R. K. (2014). Electron backscatter diffraction (EBSD) study of the structure and crystallography of the barnacle *Balanus amphitrite*. *JOM* **66**, 143-148.
Li, D., Scherfer, C., Korayem, A. M., Zhao, Z., Schmidt, O. and Theopold, U. (2002). Insect hemolymph clotting: evidence for interaction between the coagulation system and the prophenoloxidase activating cascade. *Insect Biochem. Mol. Biol.* **32**, 919-928.
Li, S., Liu, Y., Liu, C., Huang, J., Zheng, G., Xie, L. and Zhang, R. (2016). Hemocytes participate in calcium carbonate crystal formation, transportation and shell regeneration in the pearl oyster *Pinctada fucata*. *Fish Shellfish Immunol.* **51**, 263-270.
Loof, T. G., Schmidt, O., Herwald, H. and Theopold, U. (2011). Coagulation systems of invertebrates and vertebrates and their roles in innate immunity: the same side of two coins? *J. Innate Immun.* **3**, 34-40.
Maki, J. S., Rittschof, D., Costlow, J. D. and Mitchell, R. (1988). Inhibition of attachment of larval barnacles, Balanus amphitrite, by bacterial surface films. *Mar. Biol.* **97**, 199-206.
Maki, J. S., Rittschof, D., Schmidt, A. R. and Snyder, A. G. (1989). Factors controlling attachment of bryozoan larvae: a comparison of bacterial films and unfilmed surfaces. *Biol. Bull.* **177**, 295-302.
Maki, J. S., Ding, L., Stokes, J., Kavouras, J. H. and Rittschof, D. (2000). Substratum/bacterial interactions and larval attachment: Films and exopolysaccharides of *Halomonas marina* (ATCC 25374) and their effect on barnacle cyprid larvae, *Balanus amphitrite* Darwin. *Biofouling* **16**, 159-170.
Martin, G. G., Hose, J. E., Omori, S., Chong, C., Hoodbhoy, T. and Mckrell, N. (1991). Localization and roles of coagulogen and transglutaminase in hemolymph coagulation in decapod crustaceans. *Comp. Biochem. Physiol.* **100B**, 517-522.
Maruzzo, D., Conlan, S., Aldred, N., Clare, A. S. and Høeg, J. T. (2011). Video observation of surface exploration in cyprids of *Balanus amphitrite*: the movements of antennular sensory setae. *Biofouling* **27**, 225-239.
Maruzzo, D., Aldred, N., Clare, A. S. and Høeg, J. T. (2012). Metamorphosis in the cirripede crustacean *Balanus amphitrite*. *PLoS ONE* **7**, e37408.
Matsumura, K., Nagano, M., Kato-Yoshinaga, Y., Yamazaki, M., Clare, A. S. and Fusetani, N. (1998). Immunological studies on the settlement-inducing protein complex (SIPC) of the barnacle *Balanus amphitrite* and its possible involvement in larva-larva interactions. *Proc. R. Soc. B Biol. Sci.* **265**, 1825-1830.
Medzhitov, R. and Janeway, C. S. J. (2000). Innate immune recognition: mechanisms and pathways. *Immunol. Rev.* **173**, 89-97.
Mori, Y., Urushida, Y., Nakano, M., Uchiyama, S. and Kamino, K. (2007). Calcite-specific coupling protein in barnacle underwater cement. *FEBS J.* **274**, 6436-6446.
Mount, A. S., Wheeler, A. P., Paradkar, R. P. and Snider, D. (2004). Hemocyte-mediated shell mineralization in the eastern oyster. *Science* **304**, 297-300.
Mullineaux, L. S. and Butman, C. A. (1991). Initial contact, exploration and attachment of barnacle (*Balanus amphitrite*) cyprids settling in flow. *Mar. Biol.* **103**, 93-103.
Nagai, T. and Kawabata, S.-i. (2000). A link between blood coagulation and prophenol oxidase activation in arthropod host defense. *J. Biol. Chem.* **275**, 29264-29267.
Naldrett, M. J. and Kaplan, D. L. (1997). Characterization of barnacle (*Balanus eburneus* and *B. cenatus*) adhesive proteins. *Mar. Biol.* **127**, 629-635.

Nappi, A. J. and Christensen, B. M. (2005). Melanogenesis and associated cytotoxic reactions: applications to insect innate immunity. *Insect Biochem. Mol. Biol.* **35**, 443-459.
Nappi, A. J. and Ottaviani, E. (2000). Cytotoxicity and cytotoxic molecules in invertebrates. *BioEssays* **22**, 469-480.
Okay, O., Naghash, H. J. and Capek, I. (1995). Free-radical crosslinking copolymerization: effect of cyclization on diffusion-controlled termination at low conversion. *Polymer* **36**, 2413-2419.
Pawlik, J. R. and Hadfield, M. G. (1990). A symposium on chemical factors that influence the settlement and metamorphosis of marine invertebrate larvae: introduction and perspective. *Bull. Mar. Sci.* **46**, 450-454.
Phang, I. Y., Aldred, N., Clare, A. S. and Vancso, G. J. (2008). Towards a nanomechanical basis for temporary adhesion in barnacle cyprids (*Semibalanus balanoides*). *J. R. Soc. Interface* **5**, 397-401.
Rittschof, D., Branscomb, E. S. and Costlow, J. D. (1984). Settlement and behavior in relation to flow and surface in larval barnacles, *Balanus amphitrite* Darwin. *J. Exp. Biol.* **82**, 131-146.
Rittschof, D., Maki, J. S., Mitchell, R. and Costlow, J. D. (1986). Ion and neuropharmacological studies of barnacle settlement. *Neth. J. Sea Res.* **20**, 269-275.
Rittschof, D., Clare, A. S., Gerhart, D. J., Mary, S. A. and Bonaventura, J. (1992). Barnacle in vitro assays for biologically active substances: toxicity and settlement inhibition assays using mass cultured balanus amphitrite amphitrite darwin. *Biofouling* **6**, 115-122.
Rittschof, D., Orihuela, B., Stafslien, S., Daniels, J., Christianson, D., Chisholm, B. and Holm, E. (2008). Barnacle reattachment: a tool for studying barnacle adhesion. *Biofouling* **24**, 1-9.
Saroyan, J. R., Lindner, E. and Dooley, C. A. (1970). Repair and reattachment in the balanidae as related to their cementing mechanism. *Biol. Bull.* **139**, 333-350.
Saroyan, J. R., Lindner, E. and Dooley, C. A. (1996). *Attachment Mechanisms of Barnacles*. CA, USA: University of California Libraries.
Schmidt, O., Söderhäll, K., Theopold, U. and Faye, I. (2010). Role of adhesion in arthropod immune recognition. *Annu. Rev. Entomol.* **55**, 485-504.
Shivapooja, P., Wang, Q., Orihuela, B., Rittschof, D., López, G. P. and Zhao, X. (2013). Bioinspired surfaces with dynamic topography for active control of biofouling. *Adv. Mater.* **25**, 1430-1434.
Suderman, R. J., Dittmer, N. T., Kanost, M. R. and Kramer, K. J. (2006). Model reactions for insect cuticle sclerotization: cross-linking of recombinant cuticular proteins upon their laccase-catalyzed oxidative conjugation with catechols. *Insect Biochem. Mol. Biol.* **36**, 353-365.
Sugumaran, M. and Nelson, E. (1998). Model sclerotization studies. 4. Generation of N-acetylmethionyl catechol adducts during tyrosinase-catalyzed oxidation of catechols in the presence of N-acetylmethionine. *Arch. Insect Biochem. Physiol.* **38**, 44-52.
Terwilliger, N. B. (1999). Hemolymph proteins and molting in crustaceans and insects. *Integr. Comp. Biol.* **39**, 589-599.
Theopold, U., Li, D., Fabbri, M., Scherfer, C. and Schmidt, O. (2002). The coagulation of insect hemolymph. *Cell. Mol. Life Sci.* **59**, 363-372.
Theopold, U., Schmidt, O., Söderhäll, K. and Dushay, M. S. (2004). Coagulation in arthropods: defence, wound closure and healing. *Trends Immunol.* **25**, 289-294.
Unabia, C. R. C. and Hadfield, M. G. (1999). Role of bacteria in larval settlement and metamorphosis of the polychaete *Hydroides elegans*. *Mar. Biol.* **133**, 55-64.
Urushida, Y., Nakano, M., Matsuda, S., Inoue, N., Kanai, S., Kitamura, N., Nishino, T. and Kamino, K. (2007). Identification and functional characterization of a novel barnacle cement protein. *FEBS J.* **274**, 4336-4346.
Vacca, L. L. and Fingerman, M. (1983). The roles of hemocytes in tanning during the molting cycle: a histochemical study of the fiddler crab, uca pugilator. *Biol. Bull.* **165**, 758-777.
Vasta, G. R., Ahmed, H., Tasumi, S., Odom, E. W. and Saito, K. (2007). Biological roles of lectins in innate immunity: molecular and structural basis for diversity in self/non-self recognition. *Adv. Exp. Med. Biol.* **598**, 389-406.
Vazquez, L., Alpuche, J., Maldonado, G., Agundis, C., Pereyra-Morales, A. and Zenteno, E. (2009). Review: immunity mechanisms in crustaceans. *Innate Immun.* **15**, 179-188.
Waite, J. H. (1995). Precursors of quinone tanning: dopa-containing proteins. *Methods Enzymol.* **258**, 1-20.
Waite, J. H. and Qin, X. (2001). Polyphosphoprotein from the adhesive pads of *Mytilus edulis*. *Biochemistry* **40**, 2887-2893.
Waite, M. E. and Walker, G. (1988). The haemocytes of balanomorph barnacles. *J. Mar. Biol. Assoc. UK* **68**, 391.
Walker, G. (1971). A study of the cement apparatus of the cypris larva of the barnacle *Balanus balanoides*. *Mar. Biol.* **212**, 205-212.
Walker, G. (1973). The early development of the cement apparatus in the barnacle, *Balanus balanoides* (L.) (Crustacea: Cirripedia). *J. Exp. Mar. Biol. Ecol.* **12**, 305-314.
Wang, X.-W. and Wang, J.-X. (2013). Pattern recognition receptors acting in innate immune system of shrimp against pathogen infections. *Fish Shellfish Immunol.* **34**, 981-989.
Willis, J. H. (1999). Cuticular proteins in insects and crustaceans. *Integr. Comp. Biol.* **39**, 600-609.
Winston, G. W., Moore, M. N., Kirchin, M. A. and Soverchia, C. (1996). Production of reactive oxygen species by hemocytes from the marine mussel, *Mytilus edulis*: lysosomal localization and effect of xenobiotics. *Comp. Biochem. Physiol.* **113**, 221-229.
Yang, J., Cohen Stuart, M. A. and Kamperman, M. (2014). Jack of all trades: versatile catechol crosslinking mechanisms. *Chem. Soc. Rev.* **43**, 8271-8298.
Yule, A. B. and Walker, G. (1984). The adhesion of the barnacle, *balanus balanoides*, to slate surfaces. *J. Mar. Biol. Assoc. UK* **64**, 147-156.
Yule, A. B. and Walker, G. (1985). Settlement of balanus balanoides: the effect of cyprid antennular secretion. *J. Mar. Biol. Assoc. UK* **65**, 707-712.
Yule, A. B. and Walker, G. (1987). Adhesion in Barnacles. In *Barnacle Biology* (ed. A. J. Southward), pp. 389-402. Rotterdam: A. A. Balkema.
Zardus, J. D., Nedved, B. T., Huang, Y., Tran, C. and Hadfield, M. G. (2008). Microbial biofilms facilitate adhesion in biofouling invertebrates. *Biol. Bull.* **214**, 91-98.
Zhang, G., Fang, X., Guo, X., Li, L., Luo, R., Xu, F., Yang,, P., Zhang, L., Wang, X., Qi, H., et al. (2013). The oyster genome reveals stress adaptation and complexity of shell formation. *Nature* **490**, 49-54.